Electronic Supplementary Information (ESI)

Biomass-Derived Porous Carbon Materials with Sulfur and Nitrogen Dual-Doping for Energy Storage

Guiyin Xu, Jinpeng Han, Bing Ding, Ping Nie, Jin Pan, Hui Dou, Hongsen Li and Xiaogang Zhang*

Jiangsu Key Laboratory of Material and Technology for Energy Conversion, College of Material Science and Engineering

Nanjing University of Aeronautics and Astronautics, Nanjing, 210016, P. R. China

E-mail: *azhangxg@163.com*

Experimental Section

Preparation of CSB and ACSB

The shell of broad beans (SB) was washed with ethanol and dried at 60 °C for 12 h before use. SB as the carbon precursor was transferred to a tube furnace and was heat-treated at 800 °C for 2 h under nitrogen with a heating rate of 3 °C min^{-1}. The as-obtained sample was then thoroughly washed for several times with HCl (1 M) to remove any inorganic salts and then washed with distilled water until neutral pH. Then the sample was dried under a vacuum atmosphere at 80 °C for 12 h and the carbonization of the shell of broad beans (CSB) was obtained. CSB was dispersed in 3 M KOH ethanol solution and stirred for 6 hours (KOH/CSB weight ratio was 3). Then, the dried powder obtained by evaporating solvent was heated at 650 °C for 1 h under nitrogen with a heating rate of 3 °C min^{-1}. The activated sample was then thoroughly washed for several times with HCl (1 M) to remove any inorganic salts and then washed with distilled water until neutral pH. Finally, the activated carbon was dried under a vacuum atmosphere at 80 °C for 12 h and the chemical activation of CSB (ACSB) was obtained.

Characterization

X-ray diffraction (XRD) patterns were measured on a Bruker-AXS D8 DISCOVER. Copper Kα line was used as a radiation source with λ =0.15406 nm. Field emission scanning electron microscopy (FESEM) and transmission electron microscopy (TEM) measurements were carried out with JEOL JSM-6380LV FE-SEM and FEI TECNAI-20, respectively. Scanning transmission electronic microscope (STEM) was performed on a Tecnai G2 F30. The X-ray photoelectron spectroscopy (XPS) analysis was performed on a Perkin-Elmer PHI 550 spectrometer with Al Kα (1486.6 eV) as the X-ray source. The Raman spectra of CSB and ACSB were measured by using a Jobin Yvon HR800 confocal Raman system with a 632.8 nm diode laser excitation on a 300 line S mm^{-1} grating at room temperature. The N_2 adsorption/desorption tests were determined by Brunauer-Emmett-Teller (BET) measurements using an ASAP-2010 surface area analyzer. The pore size distribution (PSD) was derived from the desorption branch of the isotherm with the Barrett-Joyner-Halenda (BJH) method. Thermal gravimetric (TG) analysis was conducted on a TG-DSC instrument (NETZSCH STA 409 PC) under a N_2 atmosphere at a heating rate of 10 °C min^{-1} from 30 to 800 °C.

Electrochemical characterization

To measure the electrochemical properties of CSB and ACSB-based supercapacitors, the working electrodes were prepared by mixing active material (5 mg), acetylene black and polytetrafluoroethylene (PTFE) binder with a weight ratio of 85:10:5. After coating the above slurry on foamed Ni grids (1 cm×1 cm), the electrodes were dried at 60 °C for several hours before pressing under a pressure of 15 MPa. Cyclic voltammetry (CV) and galvanostatic charge/discharge were investigated on CHI 660A electrochemical workstation (Shanghai Chenhua, China) in a conventional three-electrode system with 6 M KOH aqueous solution as the electrolyte. Platinum foil and a saturated calomel electrode (SCE) were used as counter and reference electrodes.

A paste of ACSB (5 mg) mixed with acetylene black (10%) and PTFE binder (5%) was spread and pressed uniformly with a spatula onto a graphite disk electrode (0.6 cm diam). After drying, the electrode was placed as the working electrode. Galvanostatic charge/discharge was investigated on CHI 660A electrochemical workstation (Shanghai Chenhua, China) in a conventional three-electrode system with 1 M H_2SO_4 aqueous solution as the electrolyte, platinum foil as the counter electrode and SCE as the reference electrode.

The electrochemical measurements of CSB and ACSB for lithium ion batteries were carried out by galvanostatic cycling in CR2016-type coin cells. The working electrodes were prepared by a slurry coating procedure. The slurry consisted of 80 wt% active material, 10 wt% acetylene black and 10 wt% polyvinylidene fluoride (PVDF) dissolved in N-methyl pyrrolidinone (NMP), and was uniformly spread on a copper foil current collector. Finally, the electrode was dried at 110 °C overnight. Each current collector contained *ca* 2.0 mg cm^{-2} active material. Test cells were assembled in an argon-filled glove box using Li foil as the counter electrode and polypropylene (PP) film as the separator. 1 mol L^{-1} $LiPF_6$ in a mixed solvent of ethylene carbonate (EC) and dimethyl carbonate (DMC) with a volume ratio of 1:1 was used as the electrolyte. The coin cells were galvanostatically charged-discharged at different current densities between 0.01 and 3.0 V (*vs.* Li/Li^+) using a CT2001A cell test instrument (LAND Electronic Co.). CV measurements were conducted with a CHI 600A electrochemical workstation at a scan rate of 0.1 mV s^{-1} in the voltage range of 0.01 to 3.0 V (*vs.* Li/Li^+). Electrochemical impedance spectroscopy (EIS) was measured in the frequency range of 100 kHz-10 mHz with an amplitude of 5 mV. All capacity values in this article are calculated

according to the weight of CSB and ACSB.

The electrochemical measurements of ACSB for sodium ion batteries were carried out by galvanostatic cycling in CR2032-type coin cells. The working electrodes were prepared by a slurry coating procedure. The slurry consisted of 70 wt% active material, 20 wt% acetylene black and 10 wt% PVDF dissolved in NMP, and was uniformly spread on a copper foil current collector. Finally, the electrode was dried at 110 °C overnight. Each current collector contained *ca* 1.5 mg cm^{-2} active material. Test cells were assembled in an argon-filled glove box using Na metal as the counter electrode and a glass microfiber filter as the separator. The electrolyte was 1 M $NaClO_4$ dissolved in a mixture of EC and propylene carbonate (PC) with a volume ratio of 1:1. The coin cells were galvanostatically charged-discharged at a current density of 200 mA g^{-1} between 0.01 and 3.0 V (*vs.* Na/Na^+) using a CT2001A cell test instrument (LAND Electronic Co.).

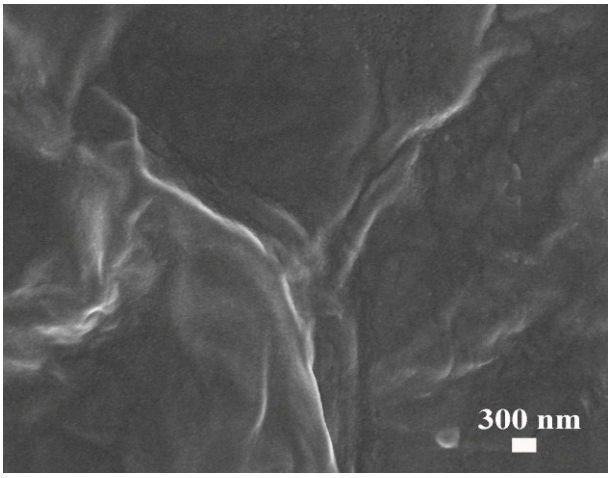

Figure S1. SEM image of CSB in the middle

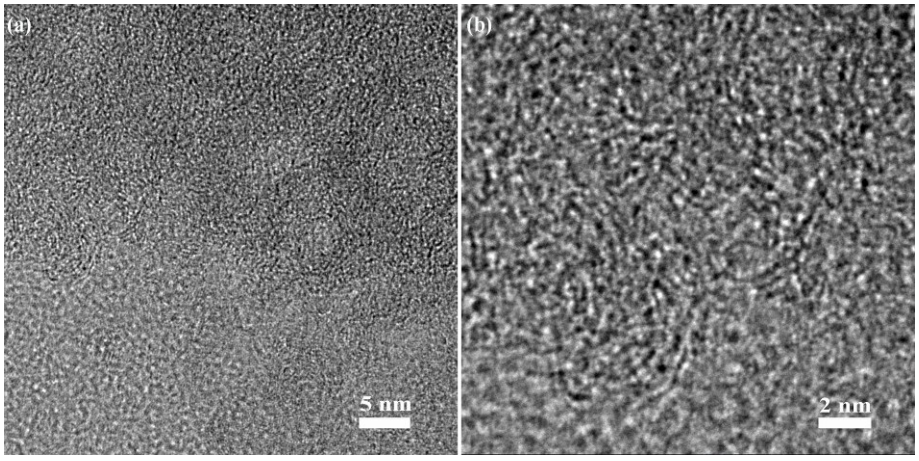

Figure S2. High-resolution transmission electron microscopy (HRTEM) images of ACSB

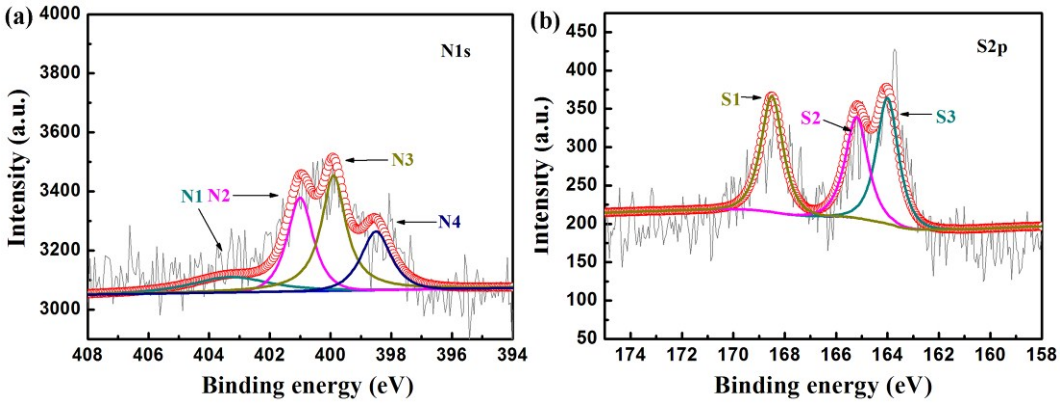

Figure S3. (a) N1s and (b) S2p XPS spectra for CSB

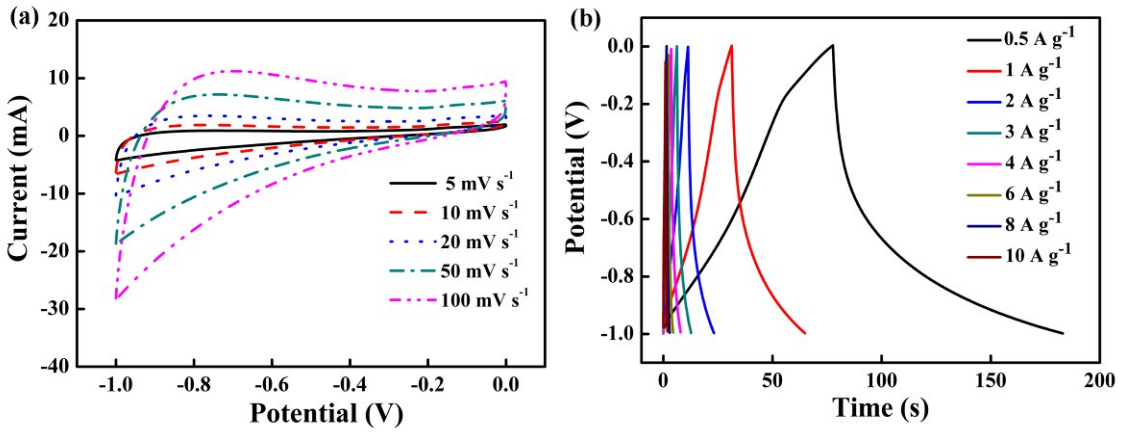

Figure S4. (a) CV curves of the CSB electrode in 6 M KOH aqueous solution at different scan rates, (b) The galvanostatic charge-discharge curves of the CSB electrode at different current densities.

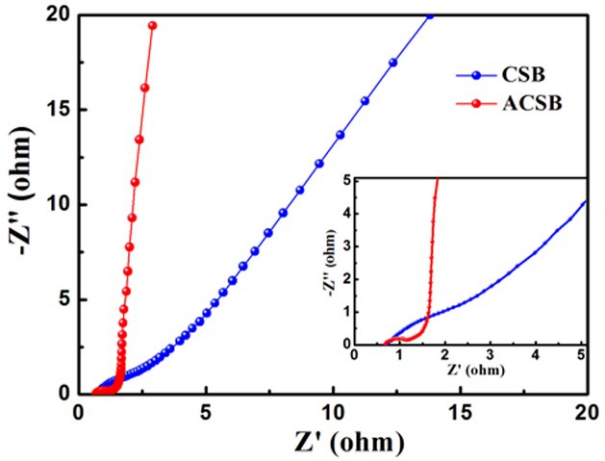

Figure S5. Impedance plots of the CSB and ACSB electrodes for electric double layer capacitors in 6 M KOH aqueous solution.

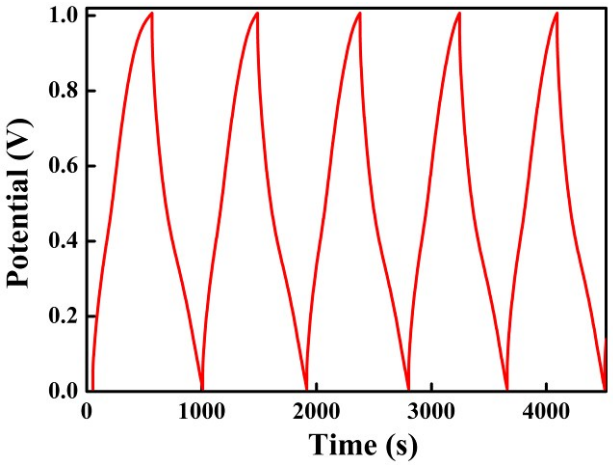

Figure S6. The galvanostatic charge-discharge curves of the ACSB electrode at a current density of 0.5 A g^{-1} in 1 M H_2SO_4 aqueous solution.

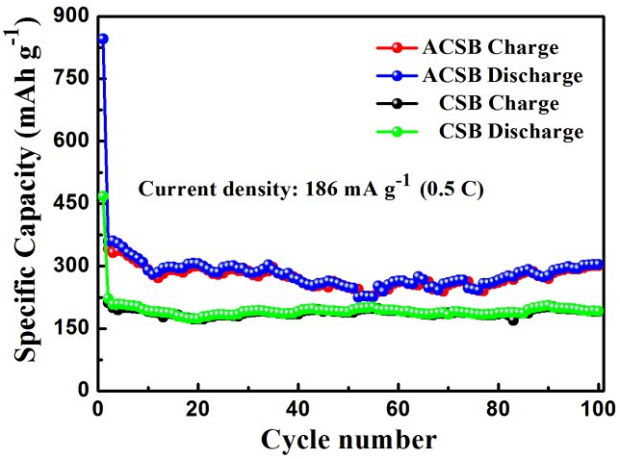

Figure S7. Cycling performance of the CSB and ACSB anodes for lithium ion batteries at a constant rate of 0.5 C

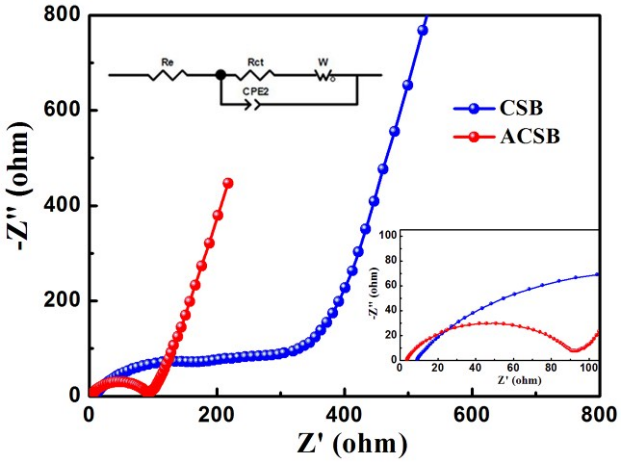

Figure S8. Impedance plots of the CSB and ACSB anodes for lithium ion batteries

Both of the spectra consist of a straight line in the low frequency region which corresponds to the ion diffusion (the Warburg impedance, W) and a semicircle in the high frequency region which relates to the interface charge-transfer process of the electrode (the charge transfer resistance, Rct).[1] The intercept at the real axis Z' represents the combination resistance (Re), which is influenced by the intrinsic resistance of the electrode materials, the ionic resistance of the electrolyte and the contact resistance of the electrode material with current collector interface. The combination resistance and the charge transfer resistance of the CSB electrode is larger than the ACSB electrode, which result from the large specific surface area, high pore volume and unique pore-size distribution for rapid electron and ion transport in the ACSB electrode.

Table S1. Composition of CSB and ACSB. The amounts of C, N, S, O (at. %) are estimated from XPS.

Samples	C	N	S	O
CSB	88.065	2.172	0.969	8.794
ACSB	87.550	2.031	0.942	9.477

Table S2. Relative amounts of nitrogen species (at. %) in CSB and ACSB

Samples	Pyridinic nitrogen (398.5 eV)	Pyrrolic nitrogen (399.9 eV)	Quaternary nitrogen (401.0 eV)	Oxidized nitrogen (403.3 eV)
CSB	19.22	40.94	26.63	13.21
ACSB	15.38	44.63	23.84	16.15

Table S3. Relative amounts of sulfur species (at. %) in CSB and ACSB

Samples	$S2p_{3/2}$ (164.0 eV)	$S2p_{1/2}$ (165.2 eV)	Oxidized sulfur (~168.5 eV)
CSB	36.43	30.11	33.46
ACSB	21.13	24.09	54.78

Table S4. Physical characteristics of CSB and ACSB

Samples	BET total surface area (m^2 g^{-1})	Total pore volume (cm^3 g^{-1})	Average pore size (nm)
CSB	10.2	0.01	4.9
ACSB	655.4	0.38	2.3

Table S5. The comparison of the specific capacitances for the CSB and ACSB electrodes

Current Density (A g^{-1})	0.5	1	2	3	4	6	8	10
CSB (F g^{-1})	53	34	24	20	17	13	11	9
ACSB (F g^{-1})	202	174	158	151	146	137	133	129

The specific capacitances are calculated from the galvanostatic charge-discharge curves based on the following equation:

$$C = \frac{I\mathrm{t}}{\mathrm{m}\Delta V}$$

where C, I, t, m and ΔV are the specific capacitance (F g^{-1}), the discharging current (A), the discharging time (s), the mass of active material (g) and the discharging potential range (V), respectively.

Table S6. Comparison of the specific capacitance of the electrodes with literature data:

Samples	Electrolyte	Capacitance (F g^{-1})	Reference
Graphene	$EMIMBF_4$ ionic liquid electrolyte	80 (8 A g^{-1})	2
66.7 wt% CNTs	1 mol L^{-1} H_2SO_4 aqueous solution	~ 90 (10 A g^{-1})	3
NCNT	6 M KOH aqueous solution	89 (10 A g^{-1})	4
PNCNT		130 (10 A g^{-1})	
PNHCS	6 M KOH aqueous solution	118 (10 A g^{-1})	5
UF-Mg-1:1	6 M KOH aqueous solution	115 (10 A g^{-1})	6
UF-Mg-1:5		123 (10 A g^{-1})	
GC-900	6 M KOH aqueous solution	~ 90 (10 A g^{-1})	7
CNS-700	BMPY TFSI ionic liquid electrolyte	~ 90 (10 A g^{-1})	8
CNS-800		~ 120 (10 A g^{-1})	

Reference

1. Y. X. Wang, L. Huang, L. C. Sun, S. Y. Xie, G. L. Xu, S. R. Chen, Y. F. Xu, J. T. Li, S. L. Chou, S. X. Dou and S. G. Sun, *J. Mater. Chem.*, 2012, **22**, 4744-4750.

2. C. Liu, Z. Yu, D. Neff, A. Zhamu and B. Z. Jang, *Nano Lett.*, 2010, **10**, 4863-4868.

3. Z. D. Huang, B. Zhang, S. W. Oh, Q. B. Zheng, X. Y. Lin, N. Yousefi and J. K. Kim, *J. Mater. Chem.*, 2012, **22**, 3591-3599.

4. G. Xu, B. Ding, P. Nie, L. Shen, J. Wang and X. Zhang, *Chem. Eur. J.*, 2013, **19**, 12306-12312.

5. J. Han, G. Xu, B. Ding, J. Pan, H. Dou and D. R. MacFarlane, *J. Mater. Chem. A*, 2014, **2**, 5352-5357.

6. X. Y. Chen, C. Chen, Z. J. Zhang, D. H. Xie and X. Deng, *Ind. Eng. Chem. Res.*, 2013, **52**, 10181-10188.

7. L. Sun, C. Tian, M. Li, X. Meng, L. Wang, R. Wang, J. Yin and H. Fu, *J. Mater. Chem. A*, 2013, **1**, 6462-6470.

8. H. Wang, Z. Xu, A. Kohandehghan, Z. Li, K. Cui, X. Tan, T. J. Stephenson, C. K. King'ondu, C. M. B. Holt, B. C. Olsen, J. K. Tak, D. Harfield, A. O. Anyia and D. Mitlin, *ACS Nano*, 2013, **7**, 5131-5141.